PERGAMON

International Journal of Heat and Mass Transfer 43 (2000) 2193–2203

International Journal of HEAT and MASS TRANSFER

www.elsevier.com/locate/ijhmt

Influence of heat conduction in the wall on nucleate boiling heat transfer

M. Mann [a], K. Stephan [a,*], P. Stephan [b]

[a] *Institut für Technische Thermodynamik und Thermische Verfahrenstechnik, Universität Stuttgart, Pfaffenwaldring 9, 70550 Stuttgart, Germany*

[b] *Fachgebiet Technische Thermodynamik, Technische Universität Darmstadt, Petersenstr. 30, 64287 Darmstadt, Germany*

Received 17 March 1999; received in revised form 2 September 1999

Abstract

On the basis of a single bubble model on heat transfer in a wedge shaped micro region the influence of heat conduction in the wall on heat transfer in nucleate boiling is studied.

The wall thermal conductivity λ_W is varied, whereas all other parameters, particularly the bubble site density, are kept constant. Wall conductivity is set to the values of copper, stainless steel and a ceramic material. The results of the parameter study show that even large variations of λ_W have only moderate influence on heat transfer to a growing vapour bubble.

Simulation results for various boiling liquids are then compared with experimental data of others to test the model and examine the influence of liquid properties upon boiling heat transfer. Although the model is based on some simplifying assumptions and thus not all heat transfer mechanisms can be described in detail, the boiling curve can be predicted in the nucleate boiling regime with good accuracy for low to moderate heat fluxes.

Keywords: Boiling; Heat transfer; Microscale

1. Introduction

Two important boiling mechanisms are likely to be influenced by the wall thermal conductivity λ_w:

- *Growth rates* of vapour bubbles, and hence heat transfer depends on the thermal conductivity λ_w of the wall.
- *Nucleation* changes for different wall conductivities. For example interactions between neighbouring sites strongly depend on the thermal conductivity of the wall material. Waiting time between two successive bubbles is also a function of the wall thermal conductivity λ_w.

The thermal conductivity of the wall can affect heat transfer coefficients via these mechanisms, Fig. 1. The effect of variations in the wall thermal conductivity λ_w on other mechanisms like enhanced convection is presumably much smaller.

The influence of thermal properties of the wall on nucleate boiling heat transfer has been studied experimentally by several authors in recent years. The following studies are of special interest for the subsequent investigations:

* Corresponding author. Tel.: +49-711-685-6106; fax: 49-711-685-7657.

E-mail address: stephan@itt.uni.stuttgart.de (K. Stephan).

0017-9310/00/$ - see front matter
PII: S0017-9310(99)00292-6

Nomenclature

a	thermal diffusivity
b	thermal penetration coefficient
c	specific heat capacity
d_{dep}	bubble departure diameter
Δh_v	enthalpy of vaporization
N_B	bubble site density
p^*	reduced pressure
$\dot{q}$	heat flux
$\dot{q}_m$	average heat flux
$\dot{q}(\xi)$	local heat flux
R_a	arithmetic mean deviation of the roughness profile
T_{sat}	saturation temperature
T_H	outside heater temperature
$T_{W,m}$	average wall temperature
$T_W(\xi)$	local wall temperature
$T_{W,mic}$	wall temperature in micro region
ΔT	$=T_{W,m}-T_{sat}$ temperature difference
Δt_B	duration of bubble growth period

Greek symbols

α_m	average heat transfer coefficient
δ	film thickness
λ	thermal conductivity
ν	kinematic viscosity
ρ	density
σ	surface tension
ξ	radial coordinate

Subscripts

co	copper
cer	ceramics
st	steel
L	liquid
V	vapour
W	wall

Braun [1] used tubes made of copper, brass and steel and determined heat transfer coefficients to boiling R12, R113 and *i*-pentane. The surface roughness parameters of the different tubes are similar. Photographs of bubble site densities for low heat fluxes (500–2000 W/m^2 for $p^*=p/p_{crit}=0.1$ on sandblasted tubes) showed significant differences in the bubble site density N_B on copper and steel tubes.

Zhou [2,3] determined heat transfer coefficients of boiling *i*-pentane and R12 on steel tubes coated with copper layers of different thickness. The active nucleation site density was far higher on thicker than on thinner copper layers, and heat transfer coefficients were up to 80% higher on the thicker layers.

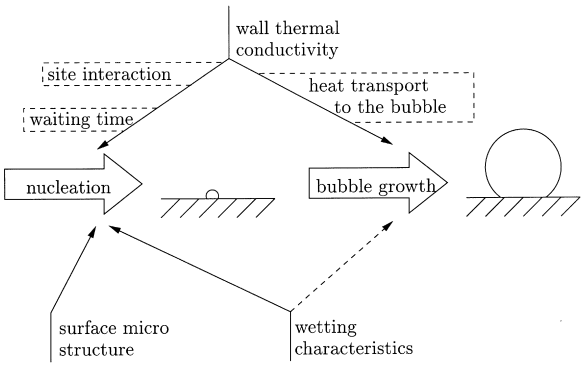

Fig. 1. Influence of wall thermal conductivity λ_W, surface micro structure and wetting characteristics on boiling mechanisms.

Magrini and Nannei [4] investigated the combined influence of wall thickness and thermal conductivity using nonmetallic rods coated with copper, silver, zinc, nickel and tin. Their experiments showed that wall thickness and thermal conductivity strongly influence nucleation site density and thereby heat transfer.

Benjamin and Balakrishnan [5] measured pool boiling heat transfer to distilled water, CCl_4, acetone and *n*-hexane on steel and aluminium surfaces. They proposed a correlation for the active nucleation site density, that includes the influence of the following thermal properties of the wall: arithmetic mean surface roughness R_a, specific heat capacity c_w, density ρ_w, thermal conductivity λ_w.

Though all these experiments delivered useful results, one should keep in mind, that replacing one wall material by another also affects other parameters than thermal conductivity, such as surface micro structure and wetting characteristics, which also influence heat transfer, Fig. 1.

As shown by Luke [6] the nucleation site density of a heater surface is not fully determined by a single roughness parameter like the arithmetic mean surface roughness R_a. We may therefore conclude, that the distribution of cavity sizes along walls of different materials can be different even if these walls have the same roughness parameters. Also the wetting characteristics, which depend for example on the oxidation of a surface influence heat transfer. Contact angle, as

shown by Wang and Dhir [7], strongly affects nucleation site density.

König [8] followed a different approach trying to avoid this combination of various effects. He used a heater with seven artificial nucleation sites, thus producing a constant bubble site density. Differences in wetting characteristics and surface micro structure of different wall materials therefore did not affect nucleation site density in his experiments. Nevertheless heat transfer coefficients from steel walls to water were lower than those from copper to water. König attributes this effect to a different contribution of convective heat transfer around the bubbles. The direct heat transfer to vapour bubbles, described by the bubble growth rate, did not much change when different wall materials were used. For heat fluxes $\dot{q}=20$ kW/m^2 and $\dot{q}=50$ kW/m^2 bubble growth times at steel walls were 13–30% longer than at copper walls.

Some efforts have been made to describe bubble growth rates by theoretical models. For example Guo and El-Genk [9] used a microlayer model to investigate bubble growth rates on heated walls of different thermal conductivities. They found a strong influence of wall thickness and thermal conductivity on bubble growth rates.

In the present paper we study the effect of wall thermal conductivity λ_w on heat flux to a single vapour bubble using the micro region model introduced by P. Stephan and Hammer [10]. Other parameters except the wall thermal conductivity, particularly the bubble site density N_B remain unchanged. The aim of this study is to clarify the influence of heat conduction in the wall upon heat transfer to vapour bubbles and to seperate it from the influence of changes in bubble site density on different wall materials.

In the simulations presented here only the influence on heat transport to a single bubble is considered while nucleation site interactions are disregarded. The model therefore is appropriate to simulate nucleate boiling heat transfer for small to intermediate heat fluxes, when interactions between bubbles are negligible. The model does not include convection due to rising bubbles which gives a significant contribution to heat transfer on horizontal tubes.

2. The model

As the model used for our computer simulation was already explained in detail in preceding publications [10,11] we confine ourselves here on a brief summary.

The model considers the fact, that a nonevaporating liquid film is adsorbed between wall and vapour bubble, Fig. 2, as shown by Wayner and co-workers [12]. Evaporation takes place in a micro region adjacent to this adsorbed film. Heat transfer and evaporation in the micro region can be described by a set of four nonlinear ordinary differential equations that are integrated to obtain the total heat transferred in the micro region.

Heat transfer in the neighbouring macro region is governed by conduction in a thermal boundary layer.

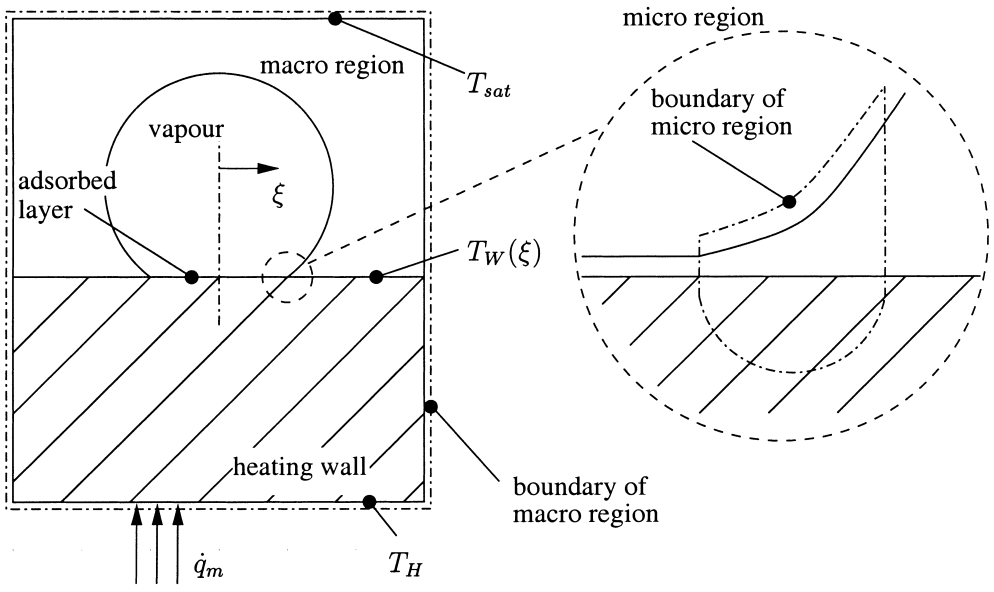

Fig. 2. The single bubble model.

This leads to partial differential equations solved numerically by a finite element method. Coupling micro and macro region yields the heat removed by a single bubble and the surrounding liquid. Thus for a given nucleation site density the overall heat transfer coefficient is obtained.

Convective heat transfer in the macro region originates from two mechanisms:

- free convection in the liquid; and
- enhanced convection caused by bubble growth and detachment.

The contribution of enhanced convection has been neglected in the model, so far. Due to this assumption there may be some uncertainties in calculated heat transfer coefficients. Nevertheless nucleate boiling heat transfer coefficients for lower to intermediate heat fluxes could be well predicted, obviously because the major effects are covered by the model.

For the bubble site densities and departure diameters experimental data of others were used. In the case of water no such data was available. Therefore a correlation proposed by P. Stephan and Hammer [13,11] was used to estimate N_B. It correlates measurements for different fluids and wall materials [14,15]. Approximate departure diameters d_{dep} for water were taken from the Fritz correlation [16]. As a sensitivity analysis revealed, errors in the departure diameter are not of great influence on calculated heat transfer coefficients. The influence is less than proportional. Therefore a good estimate of d_{dep} as given by the Fritz correlation, is considered to be sufficient for calculating heat transfer coefficients with our model at the saturation pressure considered here.

The following **modelling assumptions** are made concerning heat transfer to the bubble:

- Quasi-stationary heat transfer is assumed which means that the heat stored in the wall and the thin liquid boundary layer is neglected compared to the heat transferred by evaporation. Temperature changes with time in the energy balance are therefore neglected. The temperature field is nevertheless transient because of the moving vapour–liquid boundary. This assumption was checked by estimation of the transient contribution to the heat transferred to the bubble during a given time step, using the temperature profiles in the wall at the beginning and the end of this time step. The analysis revealed that the transient contribution is small compared to the contribution of heat conduction. In the case of R114 on a copper wall the transient contribution of the entire wall element is about 8% of the heat transferred by conduction. Near the micro region it is even less and accounts for only about 1%. On the basis of this estimation the assumption of quasi-stationary heat transfer in the copper wall is justified, all the more as the heat stored in the wall would enhance heat transfer to the bubble. The model therefore is conservative with regard to the speed of bubble growth and the overall heat transfer. In the case of R114 on a steel wall the transient contribution near the micro region is less than 3%. But in contrast to the copper wall the contribution of the whole wall element is about 50%, which is obviously significant. Therefore the calculations presented for the steel wall are very conservative and represent the worst case concerning bubble growth time and heat transfer. The same holds for the ceramic wall.
- Wall temperature along the micro region is taken to be constant. This means that the small temperature gradient in the wall parallel to the heater surface is neglected in the micro region. For the tiny micro region with a length less than 1 μm and a comparably high thermal conductivity of the wall this assumption appears reasonable. However outside of the micro region the wall temperature is not constant but a function of local position and time, and a result of the analysis.
- The temperature T_H of the wall at the boundary of the macro region opposite to the wetted surface, Fig. 2, is taken to be constant. The heat flux $\dot{q}_m$ at this boundary is a result of the analysis.

3. Results

3.1. Heat transfer in the micro region

With decreasing heat conduction in the wall, the wall temperature $T_W(\xi)$ close to the micro region decreases as well. In the micro region, the wall temperature has a minimum. Fig. 3 shows the wall temperature $T_W(\xi)$ for a bubble of given size; this is equivalent to the wall temperature after a given time. The wall temperatures are plotted for different wall materials and for the refrigerant R114 boiling at $p^* = 0.076$ and $\Delta T = 4.5$ K, as an example. Table 1 gives thermal conductivities, thermal penetration coefficients and micro region temperatures for the example in Fig. 3. The micro region wall temperature $T_{W,mic}$ located in the minimum of the temperature $T_W(\xi)$ is assumed constant, $T_W(\xi_{mic}) = T_{W,mic}$, see detail of Fig. 3. The difference in the micro region temperature $T_{W,mic}$ between a copper and a steel wall is small compared to the difference between copper and ceramics (see Table 1).

In Fig. 4 the film thickness $\delta(\xi)$ of the liquid–vapour meniscus and the heat flux $\dot{q}(\xi)$ are plotted as a func-

Table 1
Thermal conductivity, thermal penetration coefficient and wall temperature in the micro region for the example in Fig. 3 (refrigerant R114, $p^*=0.076$, $\Delta T = 4.5$ K)

Wall material	λ_W (W/(K m))	$b_W=\sqrt{\lambda_W\rho_W c_W}$ (10^3 W $s^{1/2}$/(m^2 K))	$T_{W,mic}-T_{sat}$ (K)
Copper	394	36.7	4.47
Steel	15	7.7	4.2
Ceramics	2.5	2.8	2.9

tion of the radial distance from the bubble centre in the part of the micro region directly adjacent to the adsorbed film for the same bubble size as in Fig. 3. During bubble growth the curves move along the wall and undergo only slight quantitative changes.

Further away from the adsorbed film the curvature of the meniscus is still greater than the curvature of the rest of the bubble surface but much smaller than the maximum. The boundary between the micro region and the rest of the bubble is defined as the place where the liquid–vapour interface reaches saturation temperature. This yields a micro region of about 1 μm width.

For lower wall temperatures $T_{W,mic}$ in the micro region, caused by a lower thermal conductivity of the wall, the apparent contact angle decreases, Fig. 4a. This means that the film thickness becomes smaller, and hence the thermal resistance of the liquid layer is lower, the smaller the wall thermal conductivity.

As can be seen from Fig. 4b.1 the maximum heat flux in the micro region decreases when the thermal conductivity becomes smaller. For ceramics the maximum heat flux is about 40% less than the maximum heat flux for copper. The maximum values for steel and copper differ by only 6%. To the right of the maximum, the heat fluxes for copper, steel and ceramics differ far less as can be seen in Fig. 4b.2. The difference between copper and ceramics in this region is only about 15%. This can be explained by the influence of two competing effects: First, the lower wall temperature $T_{W,mic}$ in the micro region of a low conductivity wall material causes a thinner film in the micro region, and second,

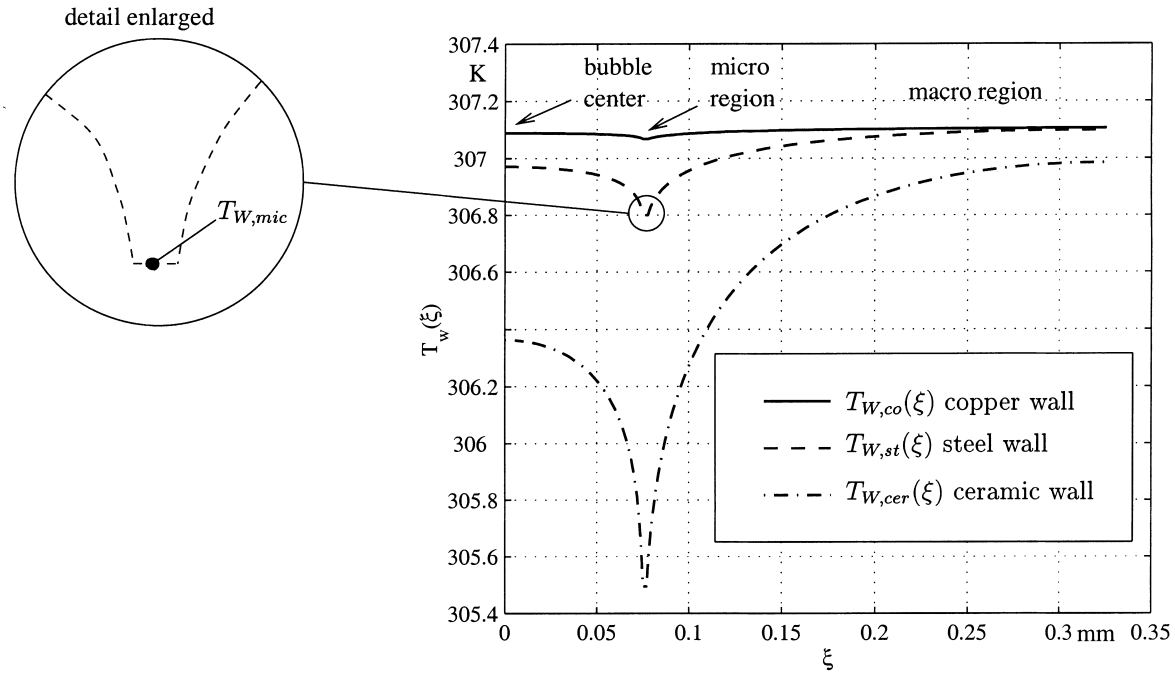

Fig. 3. Surface temperature for different wall materials $\lambda_{W,co}=394$ W/(K m), $\lambda_{W,st}=15$ W/(K m) and $\lambda_{W,cer}=2.5$ W/(K m) and the dimensions of the wall element: thickness 0.5 mm, radius 0.325 mm. Boiling R114, superheat $\Delta T=T_{W,m}-T_{sat}=4.5$ K, $p^*=0.076$.

the heat flux is lowered because of the lower wall thermal conductivity. This means that the thermal resistance in the liquid film decreases with an increase of the thermal resistance of the wall. Both effects obviously partly compensate.

In the adjacent macro region heat transfer is limited by conduction in the liquid. The wall thermal conductivity, as long as it is much higher than that of the liquid, has only a small influence on the temperature distribution in the liquid.

3.2. Nucleate boiling heat transfer coefficients

3.2.1. Different wall materials

For studying the influence of wall thermal conductivity on heat transfer we considered an artificial system. The assumptions for this system were:

- The wall thermal conductivity can be changed whereas all other properties such as surface micro structure and wetting characteristics can be kept constant.

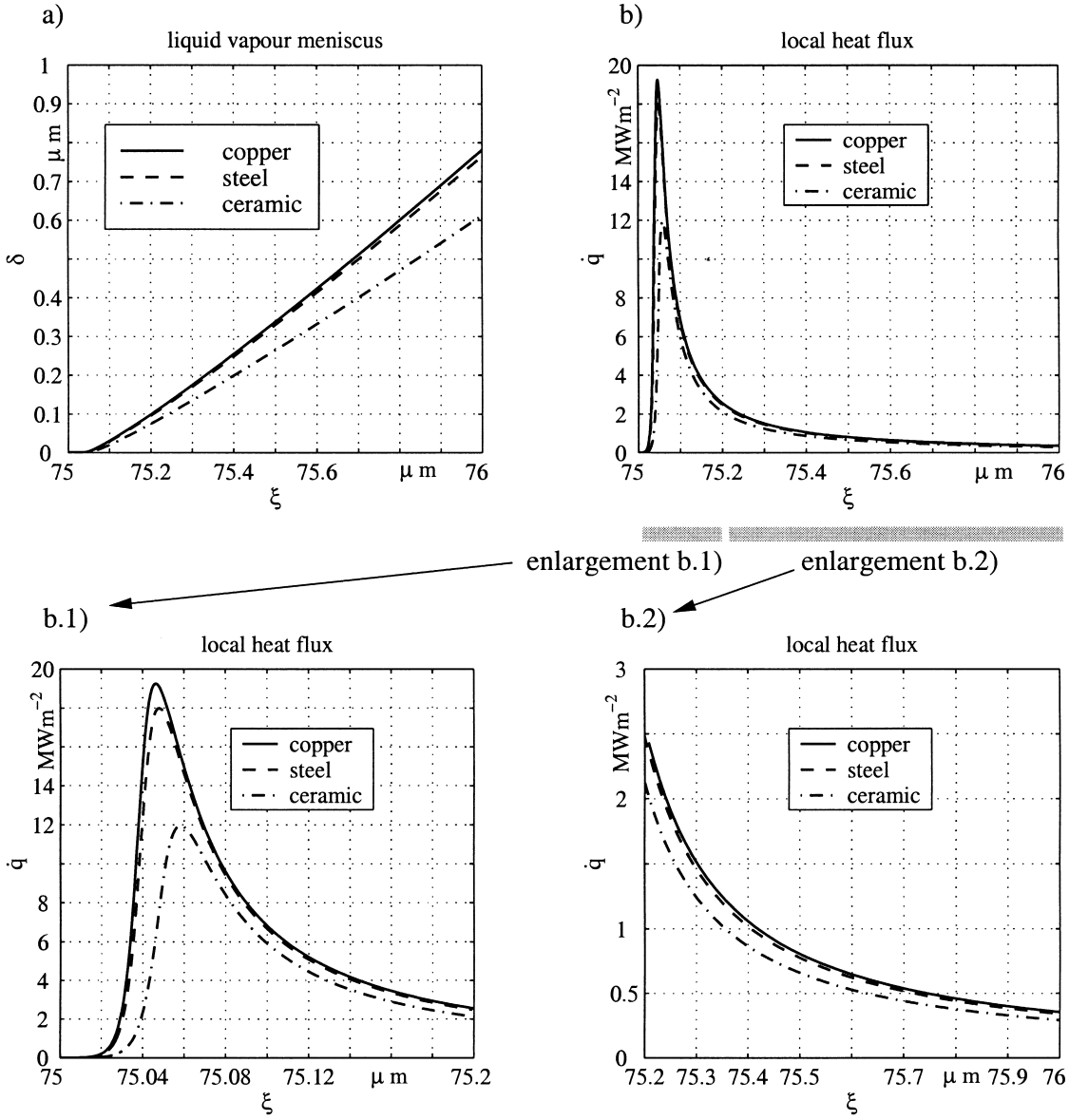

Fig. 4. Heat flux $\dot{q}(\xi)$ and film thickness (ξ) in the micro region for different wall thermal conductivities. Boiling R114, conditions as for Fig. 3.

- The bubble site density is constant for different wall thermal conductivities. This assumption is indeed a strong restriction because it presupposes that the waiting time between bubble break-off and succeeding nucleation remains unchanged. The assumption permits, however, the heat transport to a growing bubble to be investigated independently of all other influences except the wall thermal conductivity.

The boiling liquids studied are R114, propane, *i*-pentane and water. The wall materials are the same as before, namely copper, steel and ceramics.

The heat transfer coefficient is defined by

$$\alpha_m = \frac{\dot{q}_m}{\Delta T} = \frac{\dot{q}_m}{T_{W,m} - T_{sat}}, \quad (1)$$

see Fig. 2, where $\dot{q}_m$ is the average heat flux and $T_{W,m}$ the average wall temperature from nucleation to bubble departure. Both are integral mean values over time and radial coordinate.

Table 2 shows calculated heat fluxes and heat transfer coefficients of R114 for the different wall materials. The heater temperature T_H was chosen so that the temperature difference

$$\Delta T = T_{W,m} - T_{sat} \quad (2)$$

remained constant. The average heat flux $\dot{q}_m$ is a result of the calculation. As can be seen from Table 2, the heat transfer coefficient of steel differs only slightly from that of copper (~2%). Even the very low thermal conductivity of ceramics yields a comparatively high heat transfer coefficient. Although the ratio of the two wall thermal conductivities is less than 1/100,

$$\frac{\lambda_{W,st}}{\lambda_{W,co}} = 0.038, \quad \frac{\lambda_{W,cer}}{\lambda_{W,co}} = 0.0063,$$

$$\frac{b_{W,st}}{b_{W,co}} = 0.21 \approx \sqrt{\frac{\lambda_{W,st}}{\lambda_{W,co}}} = 0.20,$$

Table 2
Comparison of heat transfer to boiling R114 on walls with different thermal conductivity

Wall material	ΔT (K)	$T_H - T_{sat}$ (K)	$\dot{q}_m$ (W/m^2)	α_m (W/m^2 K)
Copper	4.48	4.50	5000	1116
Steel	4.48	4.64	4910	1095
Ceramics	4.48	5.29	4026	898

$$\frac{b_{W,cer}}{b_{W,co}} = 0.076 \approx \sqrt{\frac{\lambda_{W,cer}}{\lambda_{W,co}}} = 0.080,$$

$$\frac{a_{W,st}}{a_{W,co}} = 0.033 \approx \frac{\lambda_{W,st}}{\lambda_{W,co}} = 0.038,$$

$$\frac{a_{W,cer}}{a_{W,co}} = 0.0069 \approx \frac{\lambda_{W,cer}}{\lambda_{W,co}} = 0.0063$$

there are only moderate changes in heat transfer. The ratio of the thermal penetration coefficients b_W of the different materials is mainly given by the ratio of the wall thermal conductivities λ_W because the product $\rho_W c_W$ of density and heat capacity of the wall does not change very much for the wall materials considered. The same holds for the ratios of thermal diffusivities. Therefore the ratio of the wall thermal conductivities λ_W can be used to characterize heat transfer in the wall.

The findings for R114 also hold for propane, *i*-pentane and water as can be seen from the following summary of the simulation results:

$$\text{R114 } (p^* = 0.076) \rightarrow \frac{\alpha_{m,st}}{\alpha_{m,co}} = 0.98; \frac{\alpha_{m,cer}}{\alpha_{m,co}} = 0.80$$

$$\Delta T = 4.48 \text{ K } (N_B = 300 \text{ cm}^{-2} \text{ taken from [14]})$$

$$\text{propane } (p^* = 0.1) \rightarrow \frac{\alpha_{m,st}}{\alpha_{m,co}} = 0.97;$$

$$\Delta T = 4.48 \text{ K } (N_B = 418 \text{ cm}^{-2} \text{ taken from [17]})$$

$$\textit{i}\text{-pentane } (p^* = 0.1) \rightarrow \frac{\alpha_{m,st}}{\alpha_{m,co}} = 0.98;$$

$$\Delta T = 4.48 \text{ K } (N_B = 176 \text{ cm}^{-2} \text{ taken from [2]})$$

$$\text{water } (p^* = 0.0045) \rightarrow \frac{\alpha_{m,st}}{\alpha_{m,co}} = 0.88;$$

$$\Delta T = 8.9 \text{ K } (N_B = 16 \text{ cm}^{-2} \text{ taken from correlation})$$

These results clearly indicate, that the thermal conductivity of the wall material has little influence on the heat transport to a single bubble. For smaller superheats this influence becomes even smaller and obviously disappears near the transition to natural convection.

In real experiments, different from the artificial example considered here, the decrease in bubble site density N_B dominates, and the decrease of α_m with a

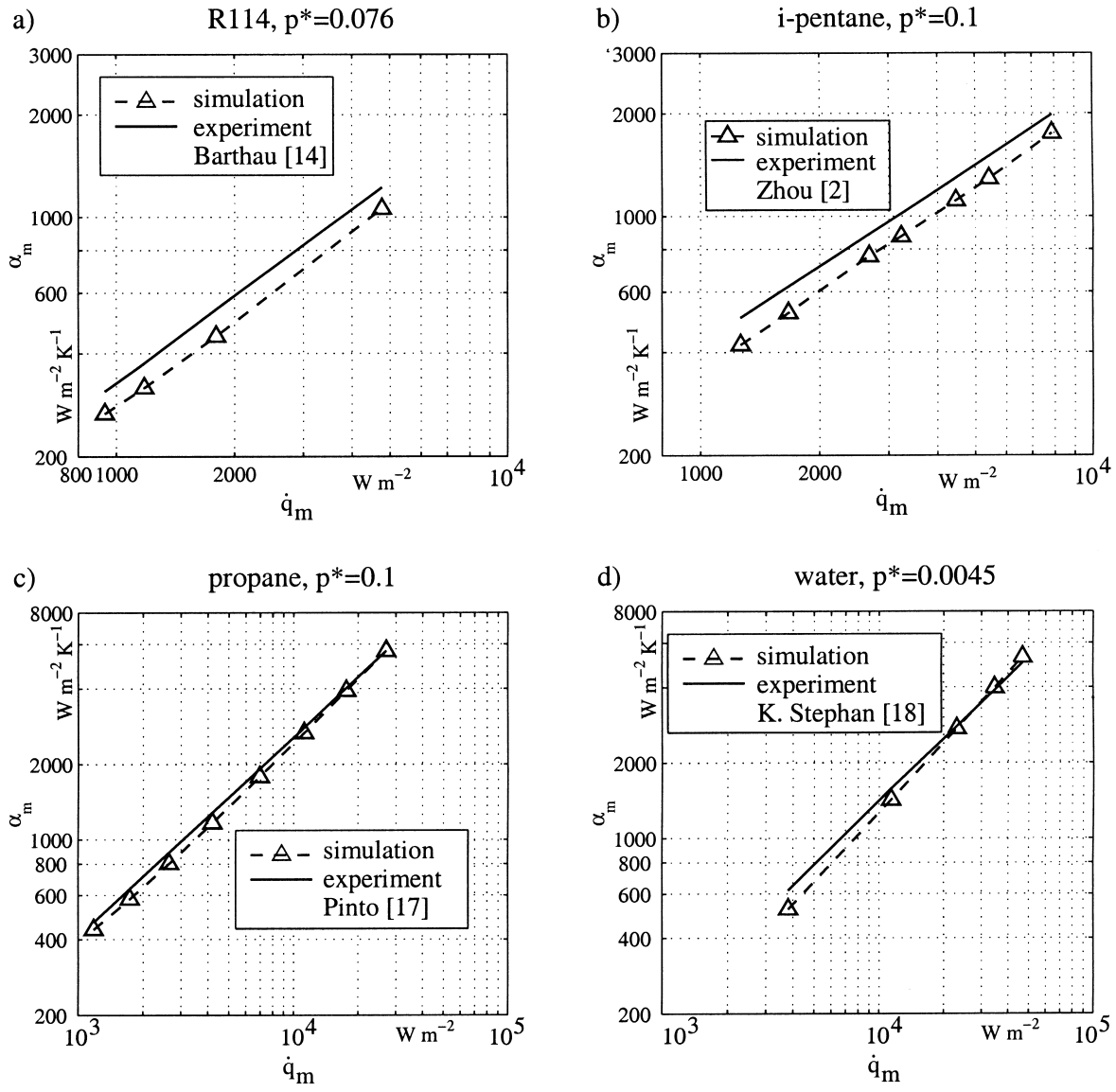

Fig. 5. Predicted heat transfer coefficients for various fluids on a copper wall compared with experimental results for horizontal tubes.

reduction of wall thermal conductivity is much higher than in our example. Braun [1] found values of $\alpha_{m,st}/\alpha_{m,co}$ between 0.56 and 0.63 for *i*-pentane at a reduced pressure $p^* = p/p_{crit} = 0.1$ on tubes of 15–16 mm diameter. Bubble site densities are obviously very sensitive to changes in the wall thermal conductivity. According to Braun bubble site densities N_B on steel walls are about 30% smaller than those on copper walls. Taking this into account in a new simulation for *i*-pentane with $N_{B,co} = 176$ cm^{-2} and $N_{B,st} = 0.7*176$ cm^{-2} $= 123$ cm^{-2}, we obtain a much higher difference between the heat transfer coefficient from steel $\alpha_{m,st}$ and from copper $\alpha_{m,co}$. The ratio becomes then

$$i\text{-pentane}\ \frac{\alpha_{m,st}}{\alpha_{m,co}} = 0.76$$

instead of the former result 0.98, and comes closer to the experimental findings 0.56 to 0.63. This result clearly indicates that the nucleation process is dominating heat transport through the wall.

For water, the influence of wall thermal conductivity on heat transfer coefficients, found in the simulation, is

also moderate. On the other hand, König found for water a much stronger decrease of heat transfer in his experiments made with a *given* number of artificial cavities. The ratio of $\alpha_{m,st}/\alpha_{m,co}$ was about 0.5 instead of the simulated value of 0.88 for the same superheat $\Delta T = 8.9$ K. König attributes this to a different contribution of convective heat transfer around the bubbles. This interpretation is supported by our simulation because the calculated growing period Δt_B between nucleation and detachment time for a bubble on a steel wall was about 17% longer than on a copper wall. For the same temperature difference König observed an increase of Δt_B of about 10%. As these results indicate that the low wall thermal conductivity of steel compared to copper is only of small influence on the heat flow to a growing bubble. Therefore the low ratio $\alpha_{m,st}/\alpha_{m,co} \approx 0.5$ found by König must be caused by another heat transfer mechanism, as for instance convection around the bubbles, not taken into account in our model.

3.2.2. Different fluids

To validate the model, heat transfer coefficients for various fluids from experiments are compared in Fig. 5 with results calculated from the model. The data of bubble formation were taken from the same experiments. The wall material was copper. The calculated heat transfer coefficients α_m for refrigerant R114, Fig. 5a, are in good agreement with experimental results of Barthau [14], who measured heat transfer, bubble density and departure diameter on a horizontal copper tube. The deviation between simulation and experiments is between 13% and 17%.

Experimental data for *i*-pentane were taken from Zhou [2] who used steel tubes coated with copper layers of different thicknesses ranging from 2 to 955 μm. Fig. 5b shows heat transfer coefficients for the copper layer of 955 μm thickness. Zhou found that the influence of the steel substrate diminishes for thick copper layers. The bubble site densities N_B observed by Zhou were comparatively small, and could only be measured for small heat fluxes. We extrapolated his values to higher wall superheats. The model predicts the experimental heat transfer coefficients α_m quite well.

While the fluid properties of propane are very similar to those of *i*-pentane, Pinto [17] found much higher bubble site densities, obviously because he used surfaces with a different micro structure. He measured the bubble site densities N_B for low, medium and high heat fluxes. Using this data as input for the model, the experimental boiling curve is predicted very well, Fig. 5c. The deviations are below 10%.

In Fig. 5d simulation results for water are compared with experiments of K. Stephan [18]. Though the bubble site density N_B could only be estimated by the empirical correlation of P. Stephan and Hammer [13,11] numerical and experimental results are in good agreement.

As can be seen from Fig. 5 the heat transfer coefficient α_m is always slightly underpredicted for low heat fluxes. A reason might be that the model neglects convection caused by bubble growth and detachment, and it does not consider the influence of bubbles rising along the surface of the horizontal tubes on heat transfer. The smaller the number of bubbles, the higher the relative effect of rising bubbles.

As Table 3 shows, refrigerant R114 has the lowest heat of vaporization of the fluids considered here. Consequently a comparatively small amount of energy is needed to produce a vapour bubble. As our parameter studies clearly indicate heat transfer increases with increasing enthalpy of vaporization Δh_v. Fig. 6 shows the influence of the enthalpy of vaporization Δh_v on heat transfer. In our simulations we augmented the enthalpy of vaporization Δh_v while all other parameters were kept constant. The corresponding reference values $\Delta h_{v,0}$ and $\alpha_{m,0}$ represent the heat of vaporization and the heat transfer coefficient of R114, propane, *i*-pentane and water, respectively. Only the points $\Delta h_v/\Delta h_{v,0} = 1$ represent real fluids. The curves in Fig. 6 represent artificial substances, to demonstrate what influence the enthalpy of vaporization Δh_v alone could have on nucleate boiling heat transfer. Heat transfer coefficients of these artificial substances are compared with those of the real fluid and the ratio $\alpha_m/\alpha_{m,0}$ is plotted against $\Delta h_v/\Delta h_{v,0}$. An exponential law for the variation found in the simulation leads to

$$\alpha_m \sim \Delta h_v^n \quad \text{with} \quad n = 0.132\text{–}0.197. \tag{3}$$

This is in good agreement with an empirical corre-

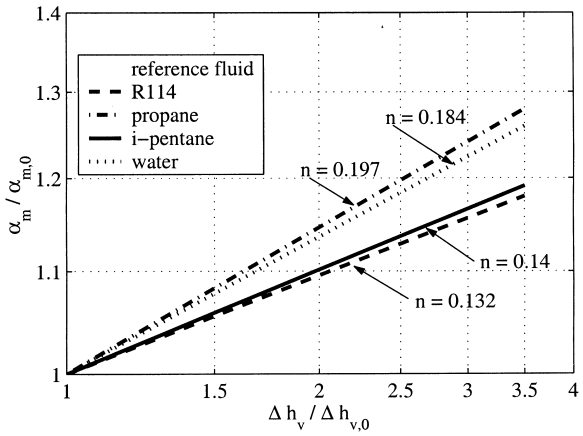

Fig. 6. Influence of enthalpy of vaporization Δh_v on heat transfer at small or moderate reduced stauration pressure.

Table 3
Physical properties of the fluids considered

Fluid properties	R114, $p^*=0.076$	Propane, $p^*=0.1$	*i*-Pentane, $p^*=0.1$	Water, $p^*=0.0045$
Δh_v (10^6 J kg^{-1})	0.13	0.38	0.31	2.26
ν_L (10^{-6} m^2 s^{-1})	0.22	0.27	0.26	0.29
$\sigma_{L,V}$ (10^{-3} N m^{-1})	10.4	11.0	9.8	58.9
λ_L (W K^{-1} m^{-1})	0.063	0.11	0.091	0.679

lation proposed by K. Stephan [18] where the exponent n turned out to be $n = 0.133$.

Fig. 7 shows temperature fields including micro and macro regions in the liquid and solid around a single bubble growing in R114 (a), propane (b) and water (c). The difference between the isotherms in the wall is $\Delta T_{iso}=0.01$ K in all three cases and in the liquid $\Delta T_{iso}=1.0$ K.

Several properties have an influence on these temperature fields. The heat of vaporization Δh_v, the viscosity ν_L, the surface tension $\sigma_{L,V}$ and the liquid thermal conductivity λ_L influence the heat transfer and fluid flow in the micro region. The temperature $T_{W,mic}$ is calculated when we couple micro and macro region. The temperature distribution in the macro region, shown in Fig. 7 therefore depends on the outside wall temperature T_H, the saturation temperature T_{sat} and the wall temperature in the micro region $T_{W,mic}$, as well as on the thermal conductivities of wall and liquid. In our cases the ratios of liquid to wall thermal conductivity were

$$\frac{\lambda_{W,co}}{\lambda_{L,R114}}=6254;\quad \frac{\lambda_{W,co}}{\lambda_{L,propane}}=3582;\quad \frac{\lambda_{W,co}}{\lambda_{L,water}}=580.$$

As Fig. 7 reveals, temperature distributions in the liquid are very similar and not strongly influenced by this ratio. The situation is different for the wall temperature distribution. The lower the ratio λ_W/λ_L, the higher is the temperature drop in the wall.

4. Summary and conclusions

In order to study the influence of thermal conductivity of the heater on nucleate boiling heat transfer a series of simulations with different thermal conductivities of the wall were performed. In this study other

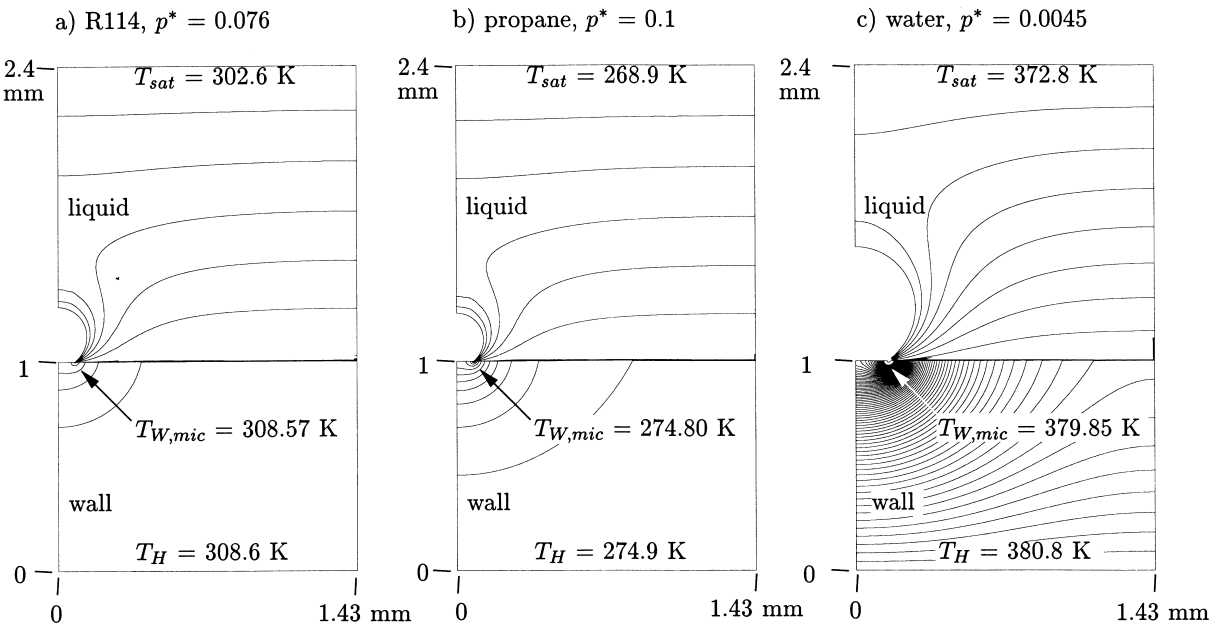

Fig. 7. Isotherms for vapour bubbles of R114, propane and water on a copper surface (temperature difference between isothermal lines inside the wall $\Delta T_{iso}=0.01$ K, inside the liquid $\Delta T_{iso}=1.0$ K).

surface parameters like wettability and surface micro structure were kept constant. Our simulations show, that the influence of wall thermal conductivity on the heat transfer in the *micro region* is small, because two effects partly compensate: The local heat flux decreases when materials with lower thermal conductivities are used. On the other hand lower thermal conductivities lead to thinner liquid films in the micro region which enhances heat conduction in the film and causes higher heat fluxes.

Nucleate boiling heat transfer coefficients of R114, *i*-pentane, propane and water on copper and steel walls were calculated with the model and compared with experiments of others. In the hypothetical case that bubble site density N_B, surface micro structure and wetting characteristics remain the same for walls with different thermal conductivities, the heat transfer coefficients on steel and copper walls do not deviate much from each other. The ratio $\alpha_{m,st}/\alpha_{m,co}$ ranges from 0.88 to 0.98 for the substances considered here. In experiments, however, smaller ratios $\alpha_{m,st}/\alpha_{m,co}$ about 0.5–0.6 were found. This is an indication, that the overall heat transfer depends more on bubble site density, which itself is influenced by different parameters, such as thermal conductivity of the wall, surface micro structure and wetting characteristics.

In order to study the influence of different fluids on the same wall material upon nucleate boiling heat transfer we calculated heat transfer coefficients for R114, *i*-pentane, propane and water on copper surfaces and compared the results with experimental data from the literature. The study of different liquids revealed that the heat transfer in the micro region is governed by several properties: the heat of vaporization Δh_v, the viscosity ν_L, the surface tension $\sigma_{L,V}$ and the liquid thermal conductivity λ_L. The temperature field in the macro region is mainly a function of the heat transferred in the micro region and the ratio λ_W/λ_L. The simulation results for the boiling curves are in good agreement with experiments.

Acknowledgements

The authors are indebted to Deutsche Forschungsgemeinschaft, Bonn, for financial assistance.

References

[1] R. Braun. Wärmeübergang beim Blasensieden an der Außenseite von geschmirgelten und sandgestrahlten Rohren aus Kupfer, Messing und Edelstahl. Diss., Universität Karlsruhe (TH), 1992.

[2] X. Zhou. Zum Einfluß des Wandmaterials auf den Wärmeübergang beim Blasensieden in freier Konvektion. Diss., Universität Karlsruhe (TH), 1995.

[3] X. Zhou, K. Bier, Influence of the heat conduction properties of the wall material and of the wall thickness on pool boiling heat transfer, in: EUROTHERM Seminar No. 48: Pool Boiling 2, Paderborn, Germany, 1996.

[4] U. Magrini, E. Nannei, On the influence of the thickness and thermal properties of heating walls on the heat transfer coefficients in nucleate pool boiling, J. Trans ASME Heat Transfer (1975) 173–178.

[5] R.J. Benjamin, A.R. Balakrishnan, Nucleation site density in pool boiling of saturated pure liquids: effect of surface microroughness and surface and liquid physical properties, Experimental Thermal and Fluid Science 15 (1997) 32–42.

[6] A. Luke, Pool boiling heat transfer from horizontal tubes with different surface roughness, Int. J. Refrig. 20 (8) (1997) 561–574.

[7] C.H. Wang, V.K. Dhir, Effect of surface wettability on active nucleation site density during pool boiling of water on a vertical surface, Trans. ASME J. Heat Transfer 115 (1993) 659–669.

[8] A. König, Der Einfluß der thermischen Heizwandeigenschaften auf den Wärmeübergang bei der Blasenverdampfung, Wärme- und Stoffübertragung 1 (1973) 38–44.

[9] Z. Guo, M.S. El-Genk, Liquid microlayer evaporation during nucleate boiling on the surface of a flat composite wall, Int. J. Heat Mass Transfer 37 (1994) 1641–1655.

[10] P. Stephan, J. Hammer, A new model for nucleate boiling heat transfer, Wärme- und Stoffübertragung 30 (1994) 119–125.

[11] J. Hammer. Einfluß der Mikrozone auf den Wärmeübergang beim Blasensieden. Diss., VDI-Verlag, 1996.

[12] P.C. Wayner, Y.K. Kao, L.V. LaCroix, The interline heat transfer coefficient on an evaporating wetting film, Int. J. Heat Mass Transfer 19 (1976) 487–492.

[13] P. Stephan, J. Hammer, Results of the micro-region model for nucleate boiling heat transfer, in: 4th UK National Conference on Heat Transfer, Manchester, 1995, pp. 283–287.

[14] G. Barthau, Active nucleation site density and pool boiling heat transfer — an experimental study, Int. J. Heat Mass Transfer 35 (1992) 271–278.

[15] V.P. Carey, Liquid–Vapor Phase-change Phenomena, Hemisphere, Washington, 1992.

[16] W. Fritz, Berechnung des Maximalvolumens von Dampfblasen, Physikalische Zeitschrift 36 (1935) 379–384.

[17] A.D. Pinto. Wärmeübergang und Blasenbildung beim Sieden von Propan an einem geschmirgelten Kupferrohr in einem groβen Druckbereich. Diss., Paderborn, 1995.

[18] K. Stephan, Beitrag zur Thermodynamik des Wärmeübergangs beim Sieden, Müller, Karlsruhe, 1964.